

No Tension Zones around Underground Openings

सिद्धिं क्तु माता मही रसा नः



Prabhat Kumar
Structural Engineering Division
Central Building Research Institute
Roorkee 247667 INDIA
Email: pbtkumar@cscbri.ren.nic.in

ABSTRACT

The concept and methodology of a NO TENSION finite element analysis was proposed more than 30 years ago. As per this methodology, the location and extent of the tension zones appear to be independent of the tensile strength properties of the medium. Also, the available strategy does not follow the standard format of a nonlinear finite element analysis. This paper proposes a finite tensile strength strategy, which overcomes both of the above limitations of the existing technology of NO TENSION analysis. At sufficiently high tensile strength, an elastic solution is obtained. The stress or strain or both criteria control may be applied to specify the tensile strength properties of the medium.

Keywords: Elasto Visco Plastic Analysis, Finite Element Analysis, Infinite Elements, Finite Tensile Strength, No tension, Rock Mechanics, Tunnels, Underground openings.

1. INTRODUCTION

The rock mass is sufficiently strong under compressive loads, however, its tensile strength is limited. In addition, the rock mass contains numerous discontinuities like joints, fissures and micro cracks which open and start propagating whenever tension develops across these. One of the major design criterion of the structures founded in or on the rock mass is to ensure that tension does not develop under the applied loads. A NO TENSION (NT) finite element analysis procedure to identify the location and extent of tension zones in a variety of structures was proposed by Zienkiewicz et al. (1968). The boundary element method was used by Venturini (1983) to perform this kind of analysis. Pande (1990) terms this kind of analysis as a time independent NO TENSION analysis and has listed its several drawbacks. A major draw-back with this existing technology is that the location and extent of the tension zones appear to be independent of the tensile strength property of the medium as it does not constitute an input. Also, the formulation of Zienkiewicz et al. (1968) is not in a standard format of nonlinear finite element analysis based on stress invariants as given by Owen and Hinton (1980). Therefore, its implementation is likely to be cumbersome.

This paper is concerned with the nonlinear finite infinite element analysis of underground openings located in a medium of known tensile strength. An elasto-visco plastic (EVP) formulation of this criterion is given which is in the standard format for a ready implementation. Some problems of underground openings are analyzed with this formulation, which clearly demonstrate the influence of available tensile strength

of the medium on the location and extent of the tension zone. It is found that for a sufficiently high tensile strength an elastic solution is obtained.

2. RANKINE CRITERION

The statement of this criterion is as follows (Chen, 1982),

$$\sigma_1 - f_t = 0 \quad (1)$$

where σ_1 is the major principal stress (in the tension positive sign convention) and f_t is the tensile strength of the medium. Chen, 1982 has also described zoning of stress, which is used in this study. The criterion given in Eq. 1 is also mentioned by Pande (1990) but with $f_t = 0$, where it is termed as time dependent no tension analysis. It appears that in-spite of ready availability of Rankine criterion, it has not been applied in the solution of real problems.

2.1 EVP Formulation

The criterion given in Eq. 1 may be expressed in terms of the alternative stress invariants proposed by Nayak and Zienkiewicz (1972) and by using the notation of Owen and Hinton, 1980, may be written as.

$$YIELD = \frac{I_1}{3.0} + \sqrt{J_2} \cdot \left(\cos \theta - \frac{\sin \theta}{\sqrt{3}} \right) \quad (2)$$

$$FDATM = f_t \quad (3)$$

where,

- I_1 = First invariant of stress tensor,
- J_2 = Second invariant of the deviatoric stress tensor,
- θ = Lode angle,
- YIELD = Computer name of yield function, and
- FDATM = Computer name of yield strength.

The derivative of yield function (Eq. 2) with respect to the stress vector which is needed in the computation of visco-plastic strains may be written as,

$$\frac{\partial Q}{\partial \sigma} = C_1 a_1 + C_2 a_2 + C_3 a_3 \quad (4)$$

$$C_1 = \frac{1}{3} \quad (5)$$

$$C_2 = \frac{\cos \theta}{2\sqrt{3} \cdot J_2} \cdot \left[(\tan 3\theta - \tan \theta) + \sqrt{3} \cdot (1 + \tan \theta \cdot \tan 3\theta) \right] \quad (6)$$

$$C_3 = \frac{\cos \theta + \sqrt{3} \cdot \sin \theta}{2J_2 \cos 3\theta} \quad (7)$$

where J_3 = Third invariant of the deviatoric stress tensor and the expressions for the coefficients a_1 , a_2 and a_3 are readily available in the published literature (Owen and Hinton, 1980).

2.2 Treatment of Corners

When the stress point lies at the corners, the direction of plastic flow vector becomes indeterminate. The Rankine criterion possesses corners at $\theta = \pm 30^\circ$. The technique suggested by Owen and Hinton (1980) has been used to deal with this situation. The coefficients C_2 and C_3 in Eqs. 6 and 7 are modified as follows,

$$\theta > 0 : C_2 = \frac{1.0}{2\sqrt{3}\sqrt{J_2}} \quad (8)$$

$$\theta < 0 : C_2 = \frac{1.0}{\sqrt{3}\sqrt{J_2}} \quad (9)$$

$$\text{and } C_3 = 0.0 \quad (10)$$

2.3 Implementation

The implemenation of this criterion in an existing nonlinear finite element analysis computer program is straight forward and follows the procedure described by Owen and Hinton (1980).

2.4 Strain Control of Tensile Strength

It is known in the context of reinforced concrete that the tensile strength of materials may be stress controlled or strain controlled (Chen, 1982). In the case of a stress control, a nonzero value of f_t in Eq. 1 is assigned and the analysis is done as usual. For a strain control, the following procedure is applied. The total effective viscoplastic strain rate at the sampling points is computed as (Owen and Hinton, 1980),

$$\bar{\epsilon}_{vp}^n = \sqrt{\frac{2}{3}} \cdot \sqrt{\dot{\epsilon}_{ij} \cdot \dot{\epsilon}_{ij}} \cdot \Delta t_n \quad (11)$$

where,

$$\begin{aligned} \Delta t_n &= \text{Current time step length, and} \\ \dot{\epsilon}_{ij} &= \text{Visco-plastic strain-rate component.} \end{aligned}$$

The strain control on the tensile strength properties of the medium can be applied by setting an appropriate value of f_t and by defining a threshold strain value ϵ_T so that when total effective VP strain rate is less than this value, it is set at zero. The setting of a non-zero but small value of ϵ_T also eliminates fictitious tensile locations created by round off errors during the iterative solution procedure.

3. NUMERICAL MODELLING REFINEMENTS

The original work of NO TENSION analysis was done more than 30 years ago. Since then, the FEM has been substantially refined. The work presented in this paper incorporated the following refinements.

- The constant strain triangular finite elements are replaced by higher order (eight node) iso-parametric finite elements, which can be numerically integrated to determine the stiffness properties. It is known that these elements can efficiently model stress gradients.
- The use of higher order elements offers another advantage in the analysis of underground excavations. The loading, which is applied on the excavation surface to eliminate the radial and shear stresses, can be more accurately simulated.
- The truncation approach is abandoned and the near and far fields of the problem are represented by the finite and infinite elements, respectively.
- The infinite elements used in this study possess an inverse type far field decay which is widely used in such applications (Kumar, 1985 and Bettess, 1992). The uniform non-zero far field decay can be accounted for without having to create nodes at infinity (Kumar, 1999). Similarly, the non-uniform nonzero far field decay is taken care of by loading the correct value of far field variable directly at the Gauss point.
- These infinite elements are to be placed sufficiently far away from the opening so that the non-linear effects do not cross the finite infinite element interface. It is also preferable to orient these infinite elements in a radial direction.

4. VERIFICATION OF FORMULATION & IMPLEMENTATION

4.1 Problem Description

The analytical derivation of the previous section and its implementation into an existing FEM analysis computer program are verified by solving the problem of a deep circular opening located in an isotropic medium. It is subjected to an internal pressure and hydrostatic initial stress field. The problem data is as follows,

$$\begin{aligned} \text{Radius of opening} &= 200.0 \text{ cm} \\ \text{Modulus of elasticity} &= 34500.0 \text{ kg/cm}^2 \\ \text{Poisson ratio} &= 0.2 \end{aligned}$$

4.2 Analytical Solution

The stress distribution around a deep circular opening is written as.

$$\sigma_r = q \left(1 - \frac{a^2}{r^2} \right) + p_i \frac{a^2}{r^2} \quad (12)$$

$$\sigma_\theta = q \left(1 + \frac{a^2}{r^2} \right) - p_i \frac{a^2}{r^2}$$

where,

$$\begin{aligned} \sigma_r \ \sigma_\theta &= \text{Radial and tangential stress,} \\ q &= \text{Strength of hydrostatic initial stress,} \\ p_i &= \text{Internal pressure,} \\ a &= \text{Radius of opening, and} \\ r &= \text{Radial distance.} \end{aligned}$$

The stress distribution given in Eq. 12 is independent of the medium properties. In the present exercise, $p_i = 3 \text{ kg/cm}^2$ and $q = 1 \text{ kg/cm}^2$ are taken. These values are designed to induce tensile tangential stress adjacent to the opening. There is no other physical significance of these values. It can be shown that for $r \leq \sqrt{2} a$, the tangential stress is tensile. It is necessary to note that the development of tensile stress is independent of the medium properties but the location and extent of no-tension zone should depend on it.

4.3 Numerical Model

The numerical model used in this study is shown in Fig. 1. This includes all the previously described refinements and contains 180 nodes. The near and far fields are described by 48 finite and 6 infinite elements, respectively. By virtue of the symmetry, only a quarter of the problem is analyzed in a plane strain formulation of the theory of elasticity.

4.4 Numerical Results

It is shown in Table 1 that the first five Gauss points located closest to the horizontal axis have tensile elastic tangential stress. In the no-tension analysis with $\epsilon_T = 0$ and $f_t = 0$, these locations are correctly identified. The size of no-tension zone would be determined by the values of ϵ_T and f_t . This problem is very well defined with a simple close form solution. The no-tension analysis reached steady state in just four iterations. The distribution of tangential stress after the no-tension analysis is interesting. The location of Gauss points with tensile stress has shifted and the magnitude of tensile stress has considerably reduced. It was found that in this range, the ordering of principal stress is upset so that the axial stress is no longer the intermediate principal stress. This analysis was repeated with a small value of Poisson ratio. It resulted in a smaller residual tensile stress and zone.

Table 1 - Numerical results of a deep circular opening in a No-Tension medium

| Element Number | Gauss Point Number | Radial Distance | Tangential Stress | | | |
|----------------|--------------------|-----------------|-------------------|---------------------|-------------|-------------------------|
| | | | Elastic value | No Tension Analysis | | |
| | | | | $\nu = 0.2$ | $\nu = 0.1$ | Plastic strain |
| 1 | 1 | 205.54 | 0.895 | -1.845 | -1.706 | 0.7355×10^{-4} |
| | 4 | 224.90 | 0.571 | -1.034 | -0.969 | 0.4684×10^{-4} |
| | 7 | 244.26 | 0.342 | -0.520 | -0.447 | 0.2808×10^{-4} |
| 7 | 1 | 255.52 | 0.225 | 0.301 | -0.192 | 0.6216×10^{-5} |
| | 4 | 274.88 | 0.053 | 0.246 | 0.166 | 0.2544×10^{-5} |
| | 7 | 294.23 | -0.076 | 0.188 | 0.148 | 0 |
| 13 | 1 | 305.50 | -0.144 | 0.102 | 0.017 | 0 |
| | 4 | 324.85 | -0.245 | -0.028 | -0.0136 | 0 |
| | 7 | 344.21 | -0.326 | -0.132 | -0.12 | 0 |
| 19 | 1 | 361.11 | -0.385 | -0.209 | -0.20 | 0 |
| | 4 | 399.82 | -0.503 | -0.361 | -0.35 | 0 |
| | 7 | 438.53 | -0.583 | -0.464 | -0.46 | 0 |
| 25 | 1 | 461.06 | -0.624 | -0.515 | -0.51 | 0 |
| | 4 | 499.78 | -0.682 | -0.590 | -0.58 | 0 |
| | 7 | 538.49 | -0.724 | -0.645 | -0.64 | 0 |

5. APPLICATION EXAMPLE

5.1 D-shaped Lined Tunnel

Problem Description - This problem was first solved by Zienkiewicz et al. (1968) and used FPS unit system. The same unit system had to be employed in this study also. The various dimensions of the problem and medium properties are available in the published literature and are not repeated here. Other than this very few details of the analysis are available.

Numerical Model - The numerical model employed in this study is shown in Fig. 2. This contains 216 nodes, 48 finite elements to describe the medium, 10 finite elements to describe lining and 8 infinite elements to model the far field. While the lining finite elements and infinite elements behave elastically, the no-tension criterion is applied to the finite elements which describe the medium.

Loading -The excavation surface is made free of the radial and shear stresses corresponding to the gravity load and horizontal stress ratio 0.2.

Numerical Results - The numerical results for $\varepsilon_T = 10^{-5}$ and a variable f_t are shown in Fig. 3. It is interesting to see how the no-tension zone reduces as f_t is increased from 400 lb/ft² (19.14 Kpa) to 1000 lb/ft² (7.85 Kpa). Only one such result was reported by Zienkiewicz et al. (1968) and from the published results it could not be determined to which value of f_t it belongs.

5.2 Deep Power House Cavern

Problem Description - The problem to be analyzed is described in Fig. 4. A very similar power house cavern was also analyzed by Zienkiewicz et al. (1968) and Venturini (1983) by FEM and BEM, respectively.

Medium Properties

| | |
|-------------------------|---------------------------------|
| Modulus of Elasticity | = 0.141 E+07 t / m ² |
| Poisson ratio | = 0.15 |
| Unit weight of material | = 2.5 t / m ³ |
| Initial stress ratio | = 0.2 |

Numerical Model - The numerical model of this problem is shown in Fig. 5. It contains 462 nodes, 130 finite elements and 24 infinite elements. In this problem, the free surface is assumed to be far away (in excess of 100 meters). This problem does not possess any symmetry and it is analyzed in a plane strain formulation.

Loading - A uniform initial stress loading is applied in which the vertical load corresponds to the weight of the overburden material between the free surface and center of the opening. These initial stresses are converted to loads on the excavation surface so as to eliminate the radial and shear stresses. A comparison of gravity load with a uniform load at the opening center shows that the uniform load is more on the top of the opening and less at the bottom by virtue of the averaging.

$$\text{Intensity of vertical initial stress} = 280 \text{ t/m}^2$$

Intensity of horizontal initial stress = 56 t/m^2

Numerical Results - The location and extent of tension zones are shown in Figs. 6a and b for tensile strength of 15 t/m^2 and 25 t/m^2 , respectively.

5.3 Discussion

Two solutions presented in this section compare very well with the published results at least in the location of the no-tension zones and their form. In addition, these solutions are more informative in that each one corresponds to a medium of a particular tensile strength. This can not be derived from the published results. A more quantitative comparison is not possible because all details of the published results are not available.

6. CONCLUDING REMARKS

The development of tensile stress in an isotropic medium may be independent of the tensile strength properties of the medium but the extent and location should depend on it. This paper gives a formulation and computation procedure so that the extent and location of no-tension zones may be linked with the tensile strength characteristics of the medium. Such characteristics may be stress or strain controlled. The correctness and effectiveness of this formulation is established in this paper through solution of three problems. The numerical models employed in this study are substantially refined in view of the recent developments in the FEM analysis.

7. ACKNOWLEDGEMENT

This paper is published with the permission of the Director of Central Building Research Institute, Roorkee. This research was supported through grant no. 3/92 from the Indian National Committee on Rock Mechanics and Tunneling Technology, Ministry of Water Resources, New Delhi.

References

- Chen, W. F. (1982). *Plasticity in Reinforced Concrete*, McGraw Hill Book Company, USA.
- Kumar, P. (1985). Static infinite element formulation, *Journal of Structural Engineering*, (ASCE), Vol. 111, ST11, pp. 2355-2372.
- Kumar, P. (1999). FEM Computations in Unbounded Domains with Non-Zero but Uniform Far Field Decay, *Computer and Structures* (in Press).
- Nayak, G. C. and Zienkiewicz, O. C. (1972). Convenient Form of Stress Invariants for Plasticity, *Journal of Structural Engineering* (ASCE), Vol.98, ST4, pp. 949-953.
- Owen, D. R. J. and Hinton, E. (1980). *Finite Elements in Plasticity: Theory and Practice*, Pine Ridge Press, Swansea, U. K.
- Pande, G. N. (1990). *Numerical Methods in Rock Mechanics*, John Wiley & Sons, U. K.
- Venturini, W. S. (1983). *Boundary Element Methods in Geo-mechanics*, Lecture Notes in Engineering, No. 4, Springer Verlag Publication.
- Zienkiewicz, O. C., King, I. P. and Valliappan, S. (1968). Stress Analysis of Rock as a No-Tension Material, *Geotechnique*, Vol. 18, pp. 56-66.

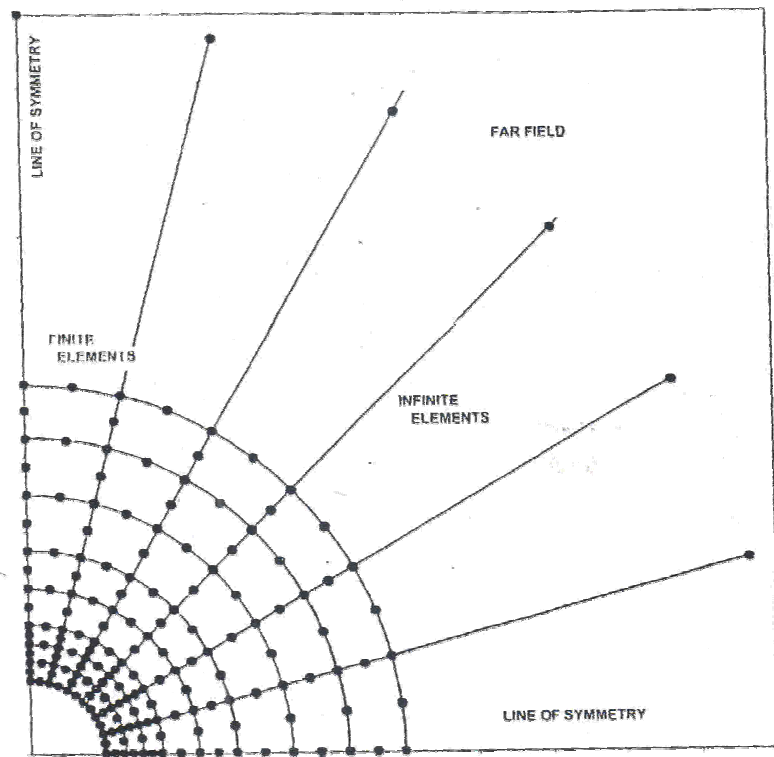


Fig. 1- Numerical model of a deep circular opening in a 'No Tension Medium'

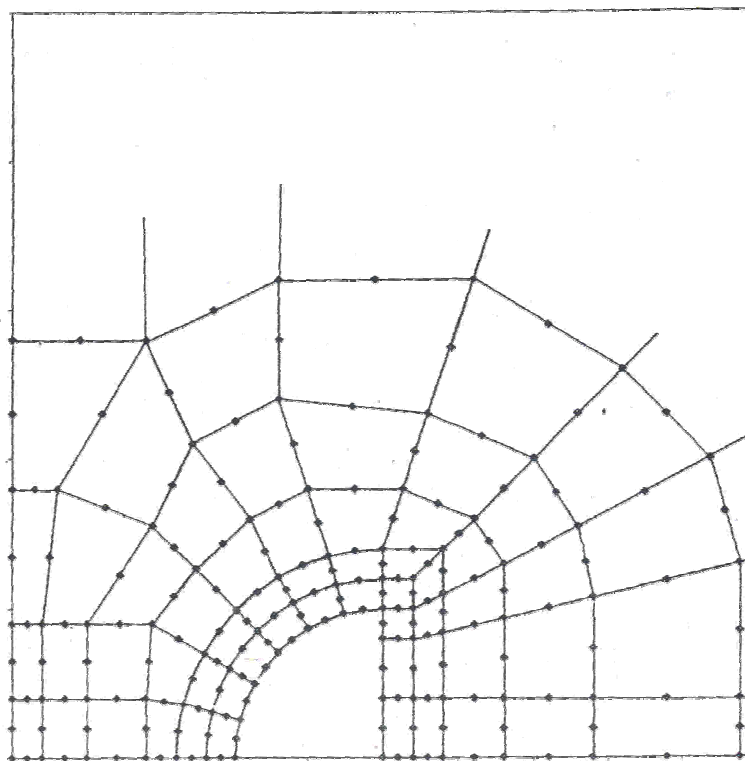


Fig. 2 - Numerical model of a D-shaped lined tunnel

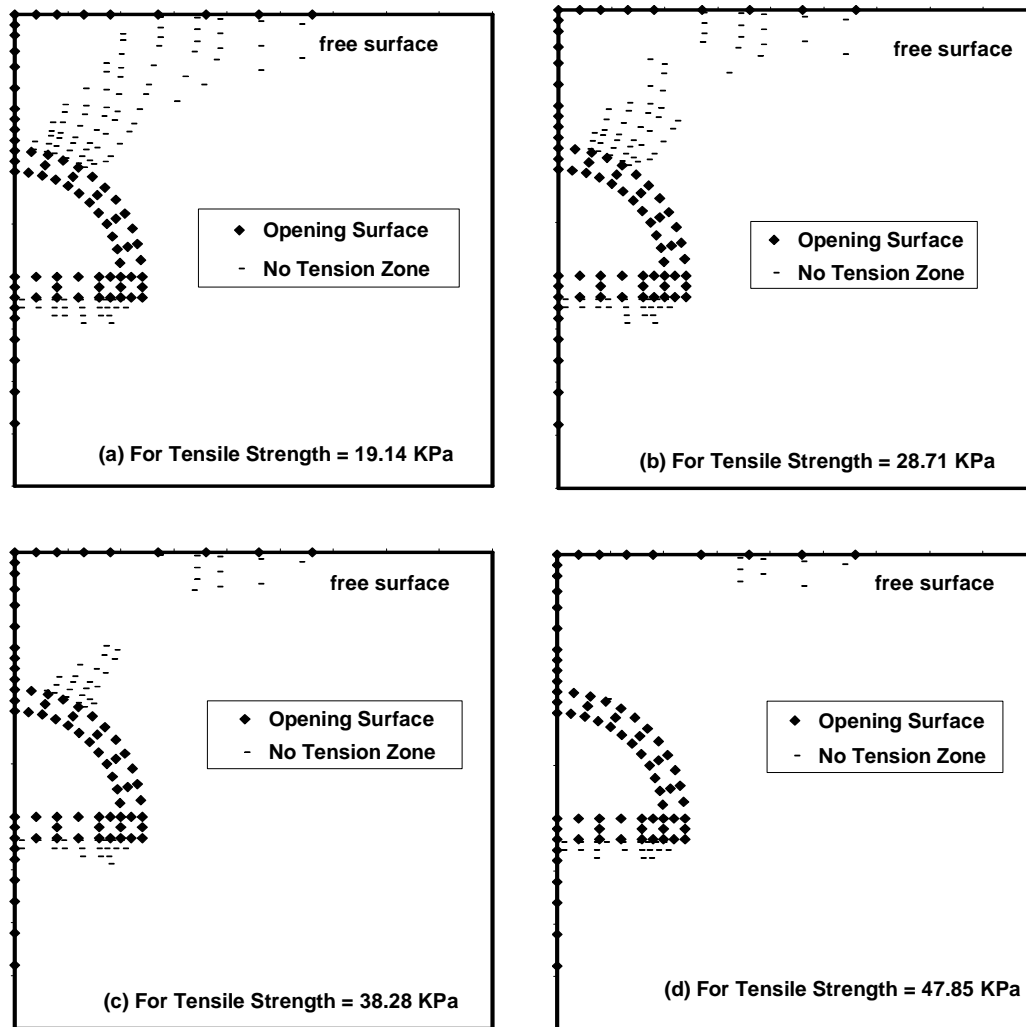


Fig. 3 No-Tension solutions of D-shaped lined tunnel (a) $f_t = 400 \text{ Lb/ft}^2$ (19.14 Kpa), (b) $f_t = 600 \text{ Lb/ft}^2$ (28.71 Kpa), (c) $f_t = 800 \text{ Lb/ft}^2$ (38.28 Kpa), and (d) $f_t = 1000 \text{ Lb/ft}^2$ (47.85 Kpa)

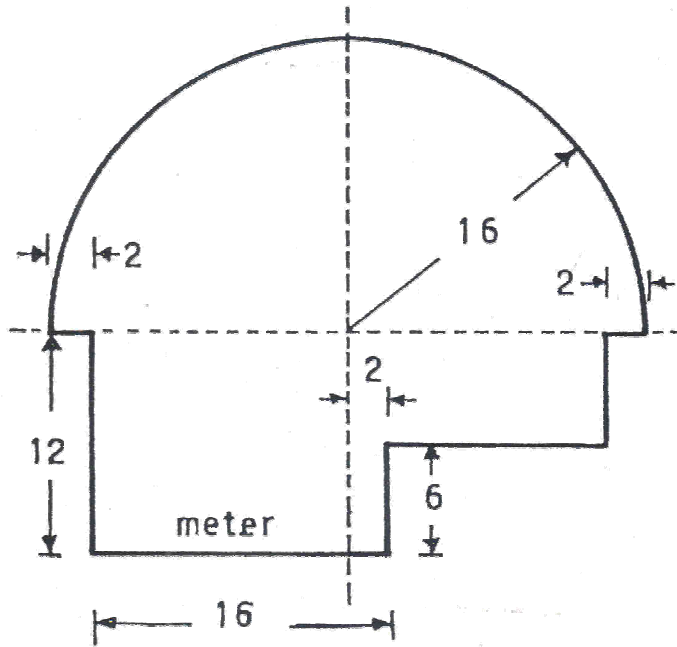


Fig. 4 – Geometry of an underground power house cavern

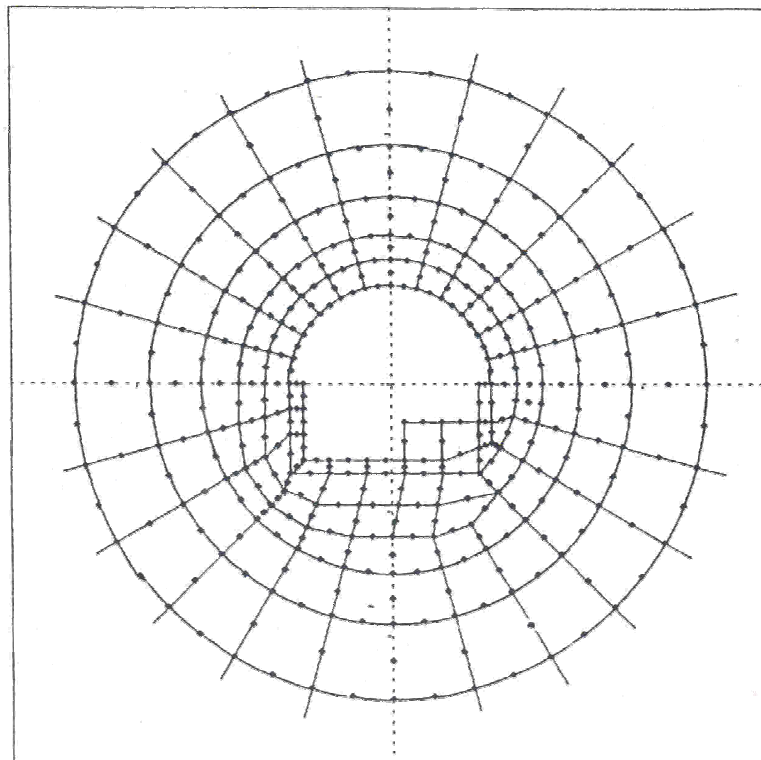


Fig. 5 – Numerical model of a deep power house cavern

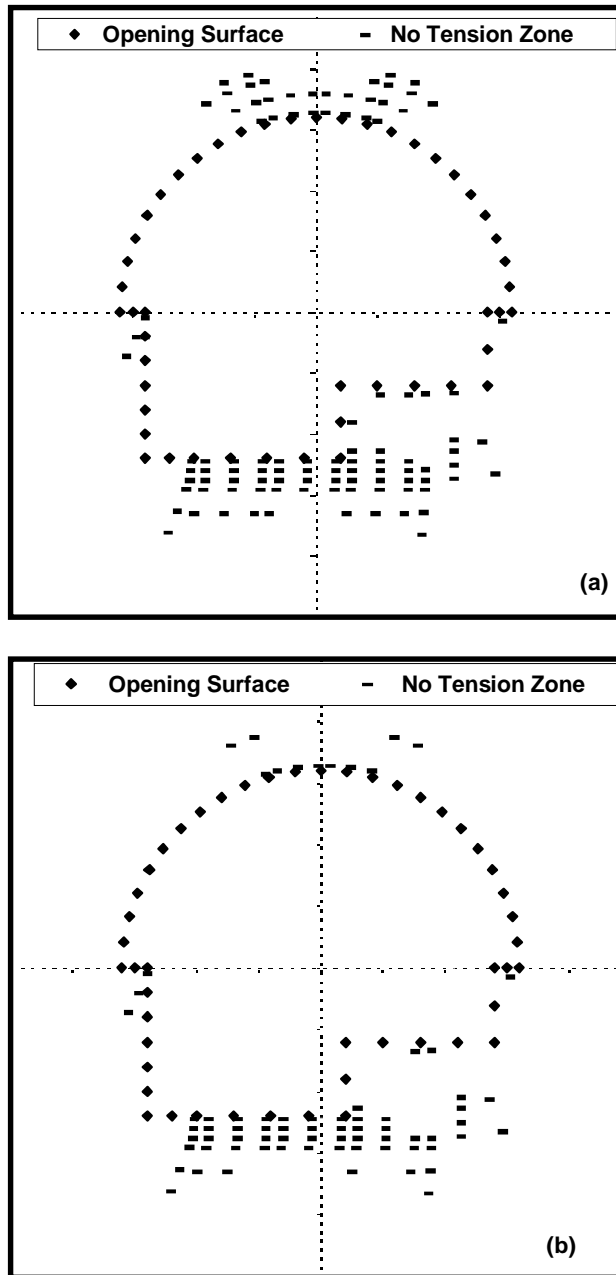


Fig. 6 - No Tension zones around the underground power house cavern
(a) Tensile strength $f_t = 15 \text{ t/m}^2$, (b) $f_t = 25 \text{ t/m}^2$